FERMILAB-Conf-03/487-AD September 2004

Angular Momentum Measurement of the FNPL Electron Beam

Y. Sun*, K.-J. Kim†, University of Chicago, Chicago, IL 60637, USA
P. Piot, K. Desler‡, D. Edwards, H. Edwards, M. Huening, J. Santucci, FNAL, Batavia, IL 60510, USA
N. Barov, D. Mihalcea, Northern Illinois University, DeKalb, IL 60115, USA
R. Tikhoplav, University of Rochester, Rochester, NY 14627, USA
S. Lidia, LBNL, Berkeley, CA 94720, USA
S.-H. Wang, Indiana University, IN 47405, USA

Abstract

In the flat beam experiment at Fermilab/NICADD Photoinjector Laboratory(FNPL)[1], it is essential to have a non-vanishing longitudinal magnetic field on the photocathode. The canonical angular momentum of the electron beam generated by this magnetic field is an important parameter in understanding the round to flat beam transformation. In this paper, we report our measurements of the canonical angular momentum, which is directly related to the skew diagonal elements of the beam matrix before beam is made flat. The measurements of the other elements of the beam matrix are also reported.

THEORY

The round-to-flat beam transformation was proposed by Brinkmann, Derbenev, and K. Flöttmann[2] based on the idea of flat-to-round transformation by Derbenev[3]. An extensive theoretical treatment of the transformation was given by Burov, Nagaitsev and Derbenev[4]. Here we summarize the main results obtained in these papers by using an approach based on the rotational symmetry and two associated invariants of the beam matrix[5].

Rotationally Invariant Beam Matrix

The coordinates of a particle in transverse phase space can be denoted by two vectors:

$$X \equiv \begin{bmatrix} x \\ x' \end{bmatrix} \text{ and } Y \equiv \begin{bmatrix} y \\ y' \end{bmatrix}. \quad (1)$$

The corresponding 4×4 beam matrix is then defined by

$$\Sigma = \begin{bmatrix} \langle XX^T \rangle & \langle XY^T \rangle \\ \langle YX^T \rangle & \langle YY^T \rangle \end{bmatrix}. \quad (2)$$

Let R be the 4×4 rotation matrix :

$$R = \begin{bmatrix} I \cdot \cos\theta & I \cdot \sin\theta \\ -I \cdot \sin\theta & I \cdot \cos\theta \end{bmatrix}, \quad (3)$$

with I standing for the 2×2 identity matrix. The beam matrix is rotationally invariant if:

$$\Sigma = R \cdot \Sigma \cdot R^{-1}. \quad (4)$$

The most general form of a rotationally invariant beam matrix is given by:

$$\Sigma = M_d \cdot \Sigma_0 \cdot M_d^T, \text{ with } \Sigma_0 = \begin{bmatrix} \varepsilon_x T & \mathcal{L}J \\ -\mathcal{L}J & \varepsilon_x T \end{bmatrix}. \quad (5)$$

where M_d is the 4×4 transfer matrix of a drift space, T and J are 2×2 matrices defined in Eq. 6, and the quantities ε_x, β and $\mathcal{L}$ are constants.

$$T \equiv \begin{bmatrix} \beta & 0 \\ 0 & \frac{1}{\beta} \end{bmatrix}, \text{ and } J \equiv \begin{bmatrix} 0 & 1 \\ -1 & 0 \end{bmatrix}. \quad (6)$$

If the beam matrix is diagonalized through some symplectic transformations, it takes the following form in the diagonalizing base:

$$\Sigma_{diag} = \begin{bmatrix} (\varepsilon_x - \mathcal{L})T_- & 0 \\ 0 & (\varepsilon_x + \mathcal{L})T_+ \end{bmatrix}, \quad (7)$$

where T_- and T_+ are diagonal matrices similar to T in Eq. 6. The beam matrix in Eq. 7 represents a flat beam which is completely decoupled in the two transverse planes with (orthogonal) transverse emittances given by:

$$\varepsilon_1 = \varepsilon_x - \mathcal{L}; \quad \varepsilon_2 = \varepsilon_x + \mathcal{L}. \quad (8)$$

The fact that rotationally invariant beam matrix has eigenvalues ε_1 and ε_2 is a general consequence of the two associated invariants: Det(Σ) and Tr($\Sigma J_4 \Sigma J_4$), where J_4 is the four dimensional unit symplectic matrix.

In the flat beam experiment at FNAL, the photocathode is immersed in a solenoidal magnetic field. Consider an electron at the photocathode surface with coordinates given by Eq. 1. The electron coordinates downstream of the solenoidal field are then given by:

$$X = \begin{bmatrix} x \\ x' - \kappa y \end{bmatrix}, \quad Y = \begin{bmatrix} y \\ y' + \kappa x \end{bmatrix}, \quad (9)$$

where $\kappa = \frac{eB_z}{2P}$, B_z is the longitudinal magnetic field on the photocathode, P is the particle momentum. From Eq. 9 and assuming there is no correlated moment at the photocathode surface (i.e. $\langle xx' \rangle = \langle xy \rangle = \ldots = 0$), the beam matrix downstream of the solenoid takes the form:

$$\Sigma_{sol} = \begin{bmatrix} A & \kappa\sigma^2 J \\ -\kappa\sigma^2 J & A \end{bmatrix}, \quad (10)$$

* yinesun@uchicago.edu
† Also APS, ANL, Argonne, IL 60439, USA
‡ Also DESY, 22603 Hamburg, Germany

where $\sigma^2 = \langle x^2 \rangle = \langle y^2 \rangle, \sigma'^2 = \langle x'^2 \rangle = \langle y'^2 \rangle$, and

$$A \equiv \begin{bmatrix} \sigma^2 & 0 \\ 0 & \kappa^2\sigma^2 + \sigma'^2 \end{bmatrix}. \quad (11)$$

The beam matrix Eq. 10 is of the form Σ_0 in Eq. 5, with the following identifications:

$$\mathcal{L} = \kappa\sigma^2,\ \varepsilon_x^2 = \varepsilon_{th}^2 + \mathcal{L}^2,\ \beta^2 = \frac{\sigma^2}{\sigma'^2 + \kappa^2\sigma^2}. \quad (12)$$

where $\varepsilon_{th} \equiv \sigma\sigma'$ is the "thermal" emittance [1]. For an angular momentum dominated beam ($\kappa\sigma \gg \sigma'$), $\beta \approx 1/\kappa$.

The beam matrix after acceleration in a rotationally symmetric structure would also be of the form given by Eq. 10, with the thermal emittance in general larger than the one on the cathode due to the space charge effect.

Conservation of Canonical Angular Momentum

The cylindrical symmetry of the system (both of the photo-emitted beam and of the externally applied fields) leads to the conservation of canonical angular momentum.

On the photocathode, the electron beam does not have any mechanical angular momentum. Thus the averaged canonical angular momentum is:

$$\langle L \rangle = eB_z\sigma^2 = 2P\mathcal{L}. \quad (13)$$

As beam propagates outside the solenoidal field, the mechanical angular momentum equals to the canonical angular momentum.

EXPERIMENTAL MEASUREMENTS

Measurement of $\mathcal{L}$

Assuming a laminar beam(i.e., neglecting the terms x' and y' in Eq. 9), the canonical angular momentum of an electron can be inferred from the observation of the beam transverse density at several locations. Indeed a measurement of the beam radii r_1 and r_2 at two locations along the beam line z_1 and z_2, together with a measurement of the shearing angle θ of the beam as it drifts between the two considered locations provides the canonical angular momentum via:

$$L = P\frac{r_1 r_2 \sin\theta}{D}, \quad (14)$$

wherein $D = z_2 - z_1$. The method is illustrated in Fig. 1.

To measure the shearing angle we intercept the beam at location z_1 with a multi-slit mask consisting of horizontal slit apertures. The thereby generated "beamlets" are then observed at the location z_2. All the beam transverse density measurements are performed using optical transition radiation (OTR) screens. An example of such measurement is illustrated in Fig. 2.

[1] Our definition of thermal emittance includes both the thermal emittance induced by the photo-emission process together with other thermalizing effects that occurs later in the transport line.

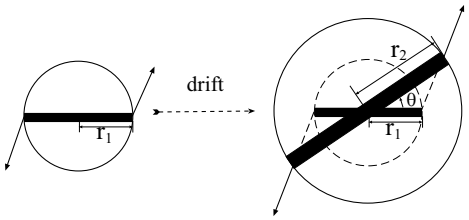

Figure 1: Beam with canonical angular momentum-induced shearing while drifting. The dark narrow rectangular can be a slit inserted into the beam line in order to measure the shearing angle.

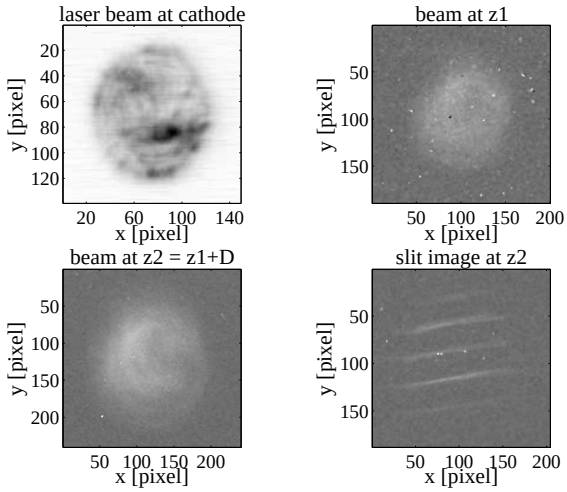

Figure 2: One set of images needed to calculate canonical angular momentum.

By observing the slit images on different OTR screens downstream, the evolution of L along the beam line can be measured. Such a measurement is plotted in Fig. 3. Within experimental error, the canonical angular momentum of an electron calculated from different screens agrees with each other. On another hand, one can measure the photocathode drive-laser beam size on the photocathode surface, this together with the knowledge of B_z, provide a measurement of L at $z = 0$, which is in good agreement with the canon-

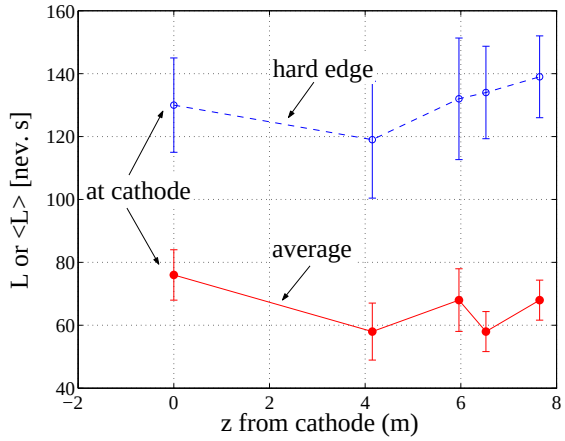

Figure 3: The canonical angular momentum of an electron: on the hard-edge of beam spot and averaged over the whole beam.

ical angular momentum computed along the beamline. In Fig. 3 we have also plotted the averaged canonical angular momentum computed from $\langle L\rangle = P\sigma_1\sigma_2 \sin\theta/D$.

Figure 3 demonstrates the canonical angular momentum is conserved for each electron in a laminar beam, thus $\langle L\rangle$ for the beam is also conserved. Given the beam energy $\sim$ 15 MeV in the experiment, we have $\mathcal{L} = \frac{\langle L\rangle}{2P} \approx 0.62\pm0.04$ mm mrad.

In a separate experiment (with a different laser spot radius), we have explored the dependence of canonical angular momentum on B_z. Our results, see Fig. 4, confirm the expected linear dependence. A linear regression of the data gives $d\langle L\rangle/dB_z = 0.08 \pm 0.02$ neV·s/G , to be compared to $d\langle L\rangle/dB_z = 0.08 \pm 0.03$ neV·s/G as evaluated from Eq. 13.

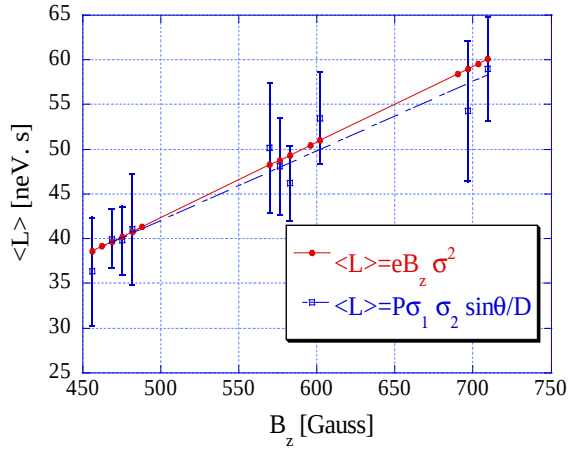

Figure 4: The averaged canonical angular momentum of an electron with different magnetic fields on the cathode.

Measurement of ε_x and β

From Eq. 5, the RMS beam envelope at location z in a drift space is given by:

$$\sigma(z) = \sqrt{\varepsilon_x\beta\left[1+\left(\frac{z-z_0}{\beta}\right)^2\right]}. \qquad (15)$$

where z_0 is the beam waist location.

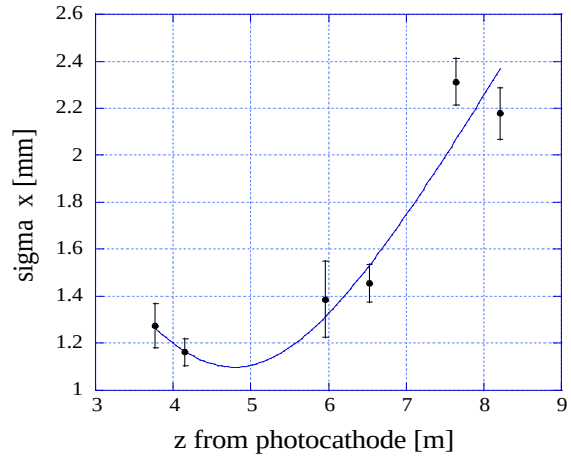

Figure 5: RMS beam envelope in a drift space.

We can measure the RMS beam size $\sigma(z)$ at different locations z in a drift space, and fit the thereby measured beam envelope to Eq. 15. From Fig. 5, we have at the beam waist location ($z_0 = 4.79 \pm 0.20$ m), $\varepsilon_x = 0.67 \pm 0.04$ mm mrad, $\beta = 1.79 \pm 0.28$ m.

Prediction of Best Possible Flat Beam Emittances

Now that $\mathcal{L}$, ε_x and β are measured, we can predict the best possible flat beam emittances one could get downstream of the round-to-flat beam transformer. From Eq. 8 we find: $\varepsilon_1 = 0.05 \pm 0.04$ mm mrad; $\varepsilon_2 = 1.29 \pm 0.04$ mm mrad. Notice that for ε_1, the error is comparable to the emittance itself.

Measurement of Flat Beam Emittances

The cylindrically symmetric beam discussed above is made flat through a skew quadrupole channel. The experimental setup is detailed in Ref. [1, 6, 7]. Our experimental conditions here differ from those in previous references, where the emphasis was put on achieving the best transverse emittance ratio. In the present experiment, however, no attempt was made to optimize the beam emittance by adjusting B_z or σ. These latter values were kept identical to those used for the measurement of L reported in Fig. 3. Note also the bunch charge ($\sim$ 1 nC) was twice as large as in Ref. [1]. The results for the *normalized* emittances are: $\varepsilon_1^n = 1.5\pm0.3$ mm mrad; $\varepsilon_2^n = 59\pm9$ mm mrad. The aforementioned errors only include the statistical errors arising from the calculation of the RMS beam or beamlet sizes.

CONCLUSIONS

The measurement of rotationally invariant beam matrix upstream of the skew quadrupole channel gives the upper limit of the achievable flat beam emittances. This allows one to do parametric studies to prepare a beam with potential to be manipulated into a flat beam with high emittance ratio, without having to actually go through the skew quadrupole channel.

REFERENCES

[1] D. Edwards *et al.*, in *Proceedings of the XX International Linac Conference*, 122 - 124 (2000).

[2] R. Brinkmann *et al.*, *Phys. Rev. ST Accel. Beams* 4, 053501 (2001).

[3] Ya. Derbenev, report UM-HE-98-04, University of Michigan (1998).

[4] A. Burov *et al.*, *Phys. Rev. E* 66, 016503 (2002).

[5] K.-J. Kim, "Notes on angular momentum dominated beam", to be published.

[6] D. Edwards *et al.*, in *Proceedings of IEEE Particle Accelerator Conference 2001*, 73 - 75 (2001).

[7] E. Thrane *et al.*, "Photoinjector Production of a Flat Electron Beam", *Proceedings of XXI International Linac Conference*, (2002).